BUBBLES IN PLANETARY NEBULAE AND CLUSTERS OF GALAXIES: JET BENDING

Noam Soker and Gili Bisker

Department of Physics, Technion−Israel Institute of Technology, Haifa 32000 Israel;
soker@physics.technion.ac.il.

ABSTRACT

We study the bending of jets in binary stellar systems. A compact companion accretes mass from the slow wind of the mass-losing primary star, forms an accretion disk, and blows two opposite jets. These fast jets are bent by the slow wind. Disregarding the orbital motion, we find the dependence of the bending angle on the properties of the slow wind and the jets. Bending of jets is observed in planetary nebulae which are thought to be the descendants of interacting binary stars. For example, in some of these planetary nebulae the two bubbles (lobes) which are inflated by the two opposite jets, are displaced to the same side of the symmetry axis of the nebula. Similar displacements are observed in bubble pairs in the center of some clusters and groups of galaxies. We compare the bending of jets in binary stellar systems with that in clusters of galaxies.

Subject headings: stars: mass loss — binaries: close — planetary nebulae: general – intergalactic medium – ISM: jets and outflows — galaxies: clusters: general

1. INTRODUCTION

The nebular gas in planetary nebulae (PNs) originates in the envelope of asymptotic giant branch (AGB) stars that are the descendants of intermediate mass stars (initial masses $\sim 1 - 8 M_\odot$). Such stars rotate very slowly, and their mass loss is expected to be spherical. Indeed, AGB stellar winds usually consist of a more or less spherically symmetric outflow at rates of $\sim 10^{-7} - 10^{-5} M_\odot$ yr^{-1}. Most PNs, though, possess a global axisymmetrical structure rather than a spherical structure in their inner region, indicating a non-spherical shaping process. Among the several PN shaping models (Balick & Frank 2002), one of the most successful is the jet-shaping model. If the jets are not well collimated they are termed collimated fast wind (CFW). The presence of jets in PNs was deduced from observations more than 20 years ago (e.g., Feibelman 1985). Gieseking et al. (1985) found collimated

outflow in the PN NGC 2392, and noted the similarity of these jets with that of young stellar objects, and speculated that such outflows exist in many similar PNs. On the theoretical side, Morris (1987) suggested that two jets blown by an accreting companion (the secondary star) can form bipolar nebulae. This model is strongly supported by the similarity of bipolar PNs to many bipolar symbiotic nebulae which are known to be shaped by jets (e.g., Schwarz et al. 1989; Corradi & Schwarz 1995). Soker (1990) proposed that the two fast low-ionization emission blobs (FLIERs or *ansae*) along the symmetry axis of many elliptical PNs are formed by jets blown during the last phase of the AGB or the post-AGB phase of the PN progenitor. The high quality HST images led Sahai & Trauger (1998) to suggest that in many PNs the non-spherical structures are formed solely by jets.

Projecting from similar astronomical objects, the formation of massive jets, to distinguish from magnetized low density pulsar jets, require the presence of accretion disks. The only source of angular momentum sufficient to form accretion disks in evolved stars is the orbital angular momentum of a stellar (or in some cases substellar) companion. The disk can be formed around the progenitor during the late post-AGB phase, when it is already small (Soker & Livio 1994), or, more likely, around a stellar companion accreting mass, forming an accretion disk, and blowing two jets.

The past seven years have seen further consolidation of the bipolar jet-shaping model in binary systems, addressed both in observations (e.g., Parthasarathy et al. 2000; Sahai & Nyman 2000; Miranda et al. 2001a,b; Corradi et al. 2001; Guerrero et al. 2001; Vinkovic et al. 2004; Huggins et al. 2004; Pena et al. 2004; Balick & Hajian 2004; Arrieta et al. 2005; Oppenheimer et al. 2005; Sahai et al. 2005) and in theory (e.g., Soker 2002, 2005; Lee & Sahai 2003, 2004; Livio & Soker 2001; Garcia-Arredondo& Frank 2004; Velazquez et al. 2004; Riera et al. 2005). Many of the PNs in the observations listed above posses point symmetric morphology, i.e., several symmetry axes rotate with respect to each other through a common origin, indicating precessing jets. The most likely explanation for precession is an accretion disk in the presence of a companion. Soker & Rappaport (2000) further discussed the jet shaping process and have shown that the statistical distribution of bipolar PNs can be accounted for in the binary model. Further support for the formation of jets in binary systems comes from X-ray observations hinting at jets in a PN (Kastner et al. 2003) similar to X-ray jets in symbiotic systems (Kellogg et al. 2001; Galloway & Sokoloski 2004). Garcia-Arredondo & Frank (2004) were the first to conduct 3D numerical simulations of the interaction of jets launched by a secondary star with the slow primary wind. Their high quality results strengthen the general stellar-binary jets model, and in particular the conjecture (Soker & Rappaport 2000) that a narrow waist can be formed by jets. It should be stressed that not all PNs are shaped by jets, but bubble pairs are formed by jets. X-ray images of active galactic nuclei in clusters of galaxies indeed show that double-jets, observed

in the radio band, can form a bubble pair with a narrow waist between them, similar to narrow waists in PNs with no need for enhanced equatorial mass loss rate, although enhanced equatorial mass loss rate might occur in many PNs.

The subject of the similarity between some morphological structures in clusters of galaxies, as revealed via X-ray observations, and in PNs, as revealed in the visible band, was studied in a series of four papers.

Paper 1 (Soker 2003b). In that paper (see also Soker 2003a, and section 5 in Soker 2004c) the similarity in morphological structures was discussed [1]. This similarity is not trivial. Two opposite jets are observed in many young stellar objects (YSOs), however, bubbles pairs similar to those in PNs and in clusters of galaxies are not usually observed around YSOs.

Paper-2 (Soker 2004a). It was found that to inflate fat, more or less spherical, bubbles the opening angle of the jets should be large; the half opening angle measured from the symmetry axis of each jet should typically be $\alpha \gtrsim 40°$, or the jets might precess.

Paper-3 (Soker 2004b). Paper 3 studies the stability of off-center low-density fat bubbles in clusters of galaxies and in PNs to the Rayleigh-Taylor instability.

Paper 4 (Pizzolato & Soker 2005). Pizzolato & Soker examined the point symmetric structure of the bubble pair in the cluster MS 0735.6+7421 (McNamara et al. 2005) and compared it to the point symmetric structure of PNs. Point symmetric PNe are thought to be shaped by stellar binary interactions; namely, the presence of a companion to the PNs progenitor star is required. Pizzolato & Soker (2005) suggested that similar point-symmetric structures in the X-ray deficient cavities of galaxy clusters might be associated with the presence of massive binary black holes.

In this paper, the fifth in the series, we examine the bending of the two jets, and the subsequent bending of the two bubbles inflated by the jets, to the same side of their original symmetry axis (jets' axis). Such displacement relative to the symmetry axis of bubbles touching the center is seen, for example, in the Perseus cluster of galaxies (Fabian et al. 2000; Dunn et al. 2006), and in the PN NGC 3587 (Guerrero et al. 2003). Dunn et al. (2006) discuss the departure of the two bubbles from their alignment along a cluster center and explain this departure by the two opposite bubbles detaching from the precessing jets at different times. We consider this displacement to result from the ram pressure of the intra cluster medium (ICM). Displacement of bubbles at a distance from the center are seen in the PN NGC 6886 (Terzian & Hajian 2000), and the group of galaxies HCG 62 (Vrtilek et al. 2002). We focus on PNs and related binary stellar objects, e.g., the massive binary stellar system η Carinae (§2.1). The departure of PNs and related binary systems from

---

[1]The similar morphologies are compared in the appendix of the astro-ph version of the present paper.

axisymmetry has been previously studied (Soker & Hadar 2002 and references therein). Our goal here is to derive a simple expression for the bending of jets in binary stellar systems (§2.2). This expression is not a substitute for future numerical simulations. The results for typical binary systems (§2.2) can account for some morphological structures in PNs and related systems. Readers interested in only using the relations and the results, can skip §2.1 and go directly to §2.2. In §3 we compare the situation with jet bending in cooling flow clusters, and §4 is a summary.

2. BENDING IN A BINARY STELLAR SYSTEM

2.1. Assumptions and Equations

When a compact secondary star accretes from the AGB (or post-AGB) stellar wind only part of the AGB wind is accreted, and the rest expands outward and forms the medium that the jets expand into. In addition, when the jet is still close to the binary system, the AGB wind hits the jet on its side, causing the jet to deflect (Soker & Rappaport 2000). Like precession, this can have large effects on the descendant PN morphology. However, while precession leads to point-symmetric nebula, the deflection of the two oppositely ejected jets is to the same side, leading the two opposite lobes to be bent to the same side; this is the *bent* departure from axisymmetry according to the classification of Soker & Hadar (2002). The bending interaction can clear the way to radiation, possibly ionizing radiation, from the central binary system to more strongly illuminate the same side in both lobes (bubbles). Due to the orbital motion, this structure forms a revolving light source. Livio & Soker (2001) suggested such a revolving ionizing source model to explain the positional shift of the bright knots in the inner nebular lobes of the M2-9 nebula (Doyle et al. 2000). Soker & Rappaport (2000) derived a simple expression for the bending angle of a narrow jet. In this section we relax some of the assumptions made by Soker & Rappaport and derive a more accurate expression for the bending angle, while still keeping the expression simple. The goal is to derive a simple approximate relation that will give the jet's bending angle upon specifying the jet's parameters and slow wind parameters.

The bending interaction is drawn schematically by Soker & Rappaport (2000) and Livio & Soker (2001), and it is shown in Figure 1; 3D images of numerical simulations are presented by Garcia-Arredondo & Frank (2004). The slow wind has a spherical mass loss rate of $\dot{M}_s$ and a relative speed to the primary star of v_s. A small fraction of this wind is accreted by the secondary star, forms an accretion disk that blows two jets, with a mass loss rate of $\dot{M}_j$ into the two jets together, and with a speed of v_j perpendicular to the equatorial plane relative to the secondary star. Although the jets can have a large opening angle and, in many cases,

are likely to have a large opening angle, in the present study we assume a narrow jet with a half opening angle $\alpha \ll 1$, and also assume that the jet is bent as one entity (sound crossing time across the jet is very short). The density per unit length along the jet axis is

$$m_j = \frac{\dot{M}_j}{2v_j} \tag{1}$$

(recall that $\dot{M}_j$ is the mass loss rate into the two jets together).

We move to a frame of reference attached to the secondary star in its orbital motion, with a velocity relative to the primary of $\mathbf{v}_{\rm orb} = v_r \hat{r} + v_\theta \hat{\theta}$, where $v_\theta \simeq r\dot{\theta}$, θ is the relative angle of the two stars in the equatorial plane, and r is the projected distance from the primary to the jet on the equatorial plane; $v_r < 0$ when the two stars approach each other. We consider a narrow jet's segment at a height z above (or below) the equatorial plane. The slow wind segment that hit this segment left the primary at an angle β to the equatorial plane (see fig. 1)

$$\sin\beta = \frac{z}{(z^2 + r^2)^{1/2}}. \tag{2}$$

The slow wind that hits the jet at a high z above the equatorial plane has a relative velocity to the jet of

$$v_{rel} = [v_\theta^2 + (v_s \cos\beta - v_r)^2 + (v_s \sin\beta)^2]^{1/2}. \tag{3}$$

We consider a fast jet $v_j \gg v_s$ that initially expands perpendicularly to the orbital plane, but is then bent by the ram pressure of the slow wind and acquires a velocity parallel to the equatorial plane v_p. The ram pressure exerted by the slow wind on the jet in a direction parallel to the equatorial plane is

$$P_{ram} = \rho \left\{ [v_\theta^2 + (v_s \cos\beta - v_r)^2]^{1/2} - v_p \right\}^2, \tag{4}$$

where the density of the slow wind

$$\rho = \frac{\dot{M}_s}{4\pi v_s (r^2 + z^2)}. \tag{5}$$

The equation for accelerating the jet in a direction parallel to the equatorial plane (perpendicular to the initial direction of the jet), under the assumption of a fast jet, $v_p \ll v_j$, reads

$$\frac{dv_p}{dt} = \frac{P_{ram} 2z \tan\alpha}{m_j} \tag{6}$$

Under the assumption of a fast jet, $z = v_j t$ and $dt = dz/v_j$. We also scale velocities by the slow wind speed

$$u_r \equiv \frac{v_r}{v_s}; \quad u_\theta \equiv \frac{v_\theta}{v_s}; \quad u_p \equiv \frac{v_p}{v_s}; \quad u_j \equiv \frac{v_j}{v_s}. \tag{7}$$
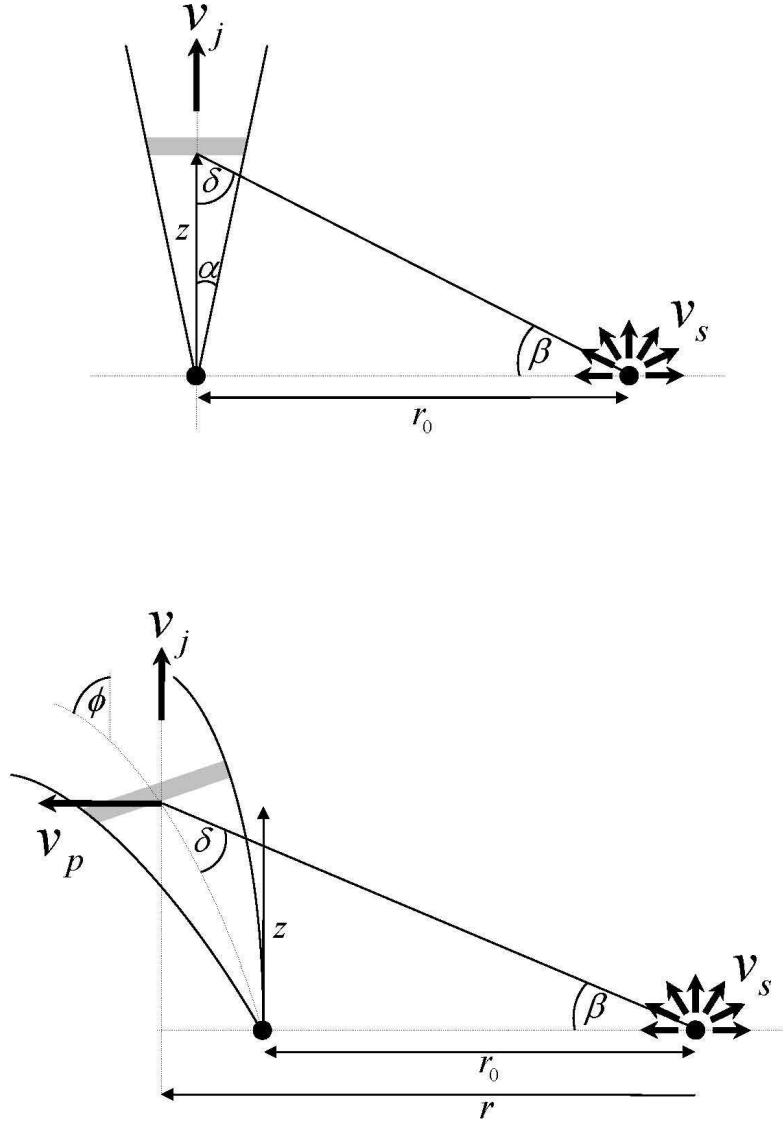
Fig. 1.— Schematic drawing of the interaction between the jet and the slow wind that bends it. The slow wind is blown at velocity v_s by the primary star on the right, while the jet is blown by the accreting secondary star on the left. The jet's speed v_j is assumed to be $v_j \gg v_s$. The mass loss rate in the two jets combined is $\dot{M}_j$, and the mass loss rate of the slow wind is $\dot{M}_s$. The orbital motion is ignored. The upper panel shows the jet when no bending occurs for clear definition of some quantities, while the lower panel show the bent jet. An opposite jet exists on the other side of the equatorial plane.

The equation of motion reads

$$\frac{du_p}{dz} = A \left\{ \left[u_\theta^2 + \left(\frac{r}{\sqrt{r^2 + z^2}} - u_r \right)^2 \right]^{1/2} - u_p \right\}^2 \frac{z}{r^2 + z^2},$$ (8)

where

$$A = \frac{\tan \alpha}{\pi} \frac{\dot{M}_s}{\dot{M}_j}$$ (9)

The meaning of the different terms in equation (8) are as follows. (1) The factor A is proportional to the ratio of colliding masses. Bending efficiency increases with A. (2) The terms u_θ and u_r result from the orbital motion of the secondary star, which blows the jets, relative to the slow wind. (3) The term $r/(r^2 + z^2)^{1/2}$ results from the ram pressure of the slow wind on the jet. The slow wind moves at a velocity v_s; but since velocity was scaled by v_s, a factor of unity multiplies this term. (4) The numerator in the last term is due to the increase in the jet cross section, and it increases the bending efficiency as the jet expands. (5) The denominator in the last term is the decrease in the slow wind density, and it makes bending less efficient as distance from the primary star grows.

2.2. Results for Impulsive Jets

We consider a case in which the jets are blown by a secondary star that is less massive than the primary star. companion. The slow wind is blown by the primary star, residing close to the center of mass of the binary system. The formulation derived above is applicable to continuously blown jets, or jets blown impulsively. However, for the bubbles in PNs, or similar object, to be significantly displaced by the mechanism discussed in §2.1, the jet should be blown during a short time compare to the orbital period. (Significant displacement from axisymmetry for continuously blown jets can be acquired if the binary system has a large eccentricity; see references in Soker & Hadar 2002.). In many PNs, the jets' ejection (PN jets refer to the jets blown by the PN progenitor) can take place over a short time period (e.g., Meaburn 2006), which we take to be shorter than the orbital period. For example, the orbital period can be 5-50 years (orbital separation of $\sim 3 - 20$ AU), and the ejection event a few years, as in symbiotic-nova outbursts on an accreting WD companion. The mass accretion rate from the primary stellar wind, $\dot{M}_2$, by a companion of mass M_2 at an orbital separation r_0 is

$$\frac{\dot{M}_2}{\dot{M}_s} \simeq 0.05 \left(\frac{M_2}{0.6M_\odot} \right)^2 \left(\frac{v_{rel}}{15 \text{ km s}^{-1}} \right)^{-4} \left(\frac{r_0}{10 \text{ AU}} \right)^{-2}.$$ (10)

If in impulsive jets' ejection $\dot{M}_j \sim 0.2\dot{M}_2$, then for the above mass accretion rate $A \simeq 5.6\alpha/10°$. In short eruption events, like disk instability or nova-like outbursts on an accreting WD, it might be that $\dot{M}_j > 0.2\dot{M}_2$, and r_0 span a range of $\sim 1 - 30$ AU. Therefore, we consider A to be be in the range $A \sim 0.1 - 100$.

The jet is bent, according to equation (8), and u_p, the velocity component parallel to the equatorial plane and perpendicular to initial velocity of the jet reaches an asymptotic velocity of

$$u_{pa} = \left[u_\theta^2 + \left(\frac{r}{\sqrt{r^2 + z^2}} - u_r \right)^2 \right]^{1/2}. \tag{11}$$

where u_{pa} is in unit of the slow wind speed v_s. The asymptotic (final) velocity u_p due to the orbital tangential velocity u_θ does not depend on the factor A or the jet speed v_j (or $u_j = v_j/v_s$). This is approximately true for the radial orbital component u_r as well, meaning that the initial jet velocity component along the secondary stellar orbital motion is quite efficiently reduced to zero. The departure from axisymmetry due to the orbital motion of the star blowing the jet will be small. Therefore, in imposing a noticeable large-scale departure from axisymmetry, where the two jets are bent to the same side, the bending due to the slow wind outflow from the primary star must be considered. This bending is less efficient because the slow wind velocity is not perpendicular to the jet velocity after the jet leaves the equatorial plane, as seen by the decreasing of the term $r/(r^2 + z^2)^{1/2}$. Ignoring the orbital motion, equation (8) reads

$$\frac{du_p}{dz} = A \left[\frac{r}{(r^2 + z^2)^{1/2}} - u_p \right]^2 \frac{z}{r^2 + z^2}, \tag{12}$$

This equation is supplemented by another equation for the jet propagation along the direction perpendicular to the equatorial plane. For a fast jet, $v_j \gg v_s$, this reads,

$$\frac{dr}{dz} = \frac{u_p}{u_j}. \tag{13}$$

Figure 2 presents the numerical solutions of the last two coupled equations for initial jet's speed $u_j \equiv v_j/v_s = 6$ and for three values of A as function of the distance from the equatorial plane z in units of the orbital separation r_0. The velocity u_p is plotted in the upper panel, in the middle panel the projection of the jet distance on the equatorial plane r is drawn (in units of r_0), while the lower panel presents the acceleration du_p/dz. In Figure 3, we show the asymptotic velocity u_{pa} as a function of A for $u_j = 6$ (the thick line).

Changing the initial jet's speed u_j does not change the solution for u_p, while the quantity $r - r_0$ is proportional to u_j^{-1}, because the bending angle is given by $\tan\phi = u_p/u_j$, so that for
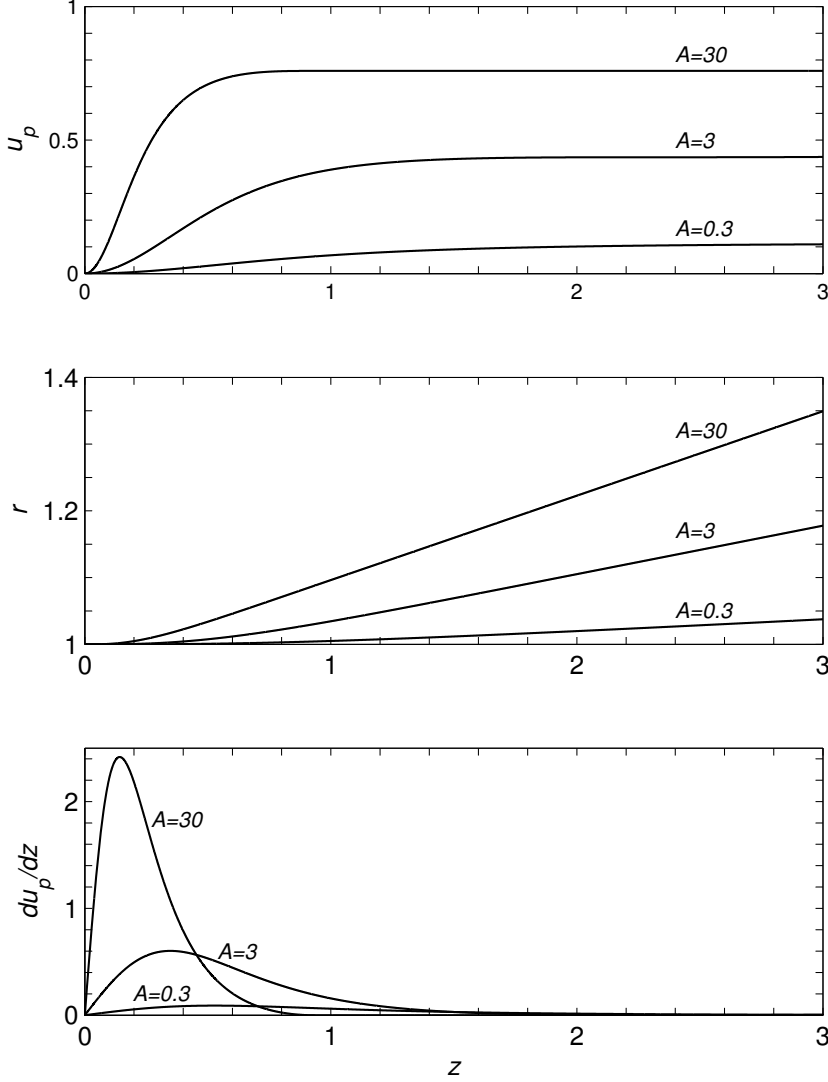
Fig. 2.— The bending properties of a jet with initial velocity, $u_j \equiv v_j/v_s = 6$, and for three values of A as defined in equation (9). The distance z form the equatorial plane is given in units of the binary orbital separation r_0. *Upper panel:* The transverse (to the initial jet velocity) jets' velocity, in units of the slow wind velocity ($u_p \equiv v_p/v_s$), obtained by solving the coupled equations (12) and (13). *Middle panel:* The projected distance on the orbital plane r in units of r_0 (see fig. 1). *Lower panel:* The transverse (bending) acceleration du_p/dz as given in equation (12).

faster jets the bending angle decreases; the dependence is $\phi \propto v_j^{-1}$. This can be understood as follows. As the jet speed v_j increases, the time of accelerating the jet by the slow wind's ram pressure along a distance dz decreases as v_j^{-1}; however, the density in the jet decreases as v_j^{-1} as well. Hence the total change in v_p (or u_p) along a distance dz does not depend on v_j under our assumptions, in particular the assumption v_j (or u_j) is constant and is not influenced by the interaction with the slow wind. As seen from Figure 2, for a fast jet (and for typical values used here) u_p almost reaches its terminal speed while $r \simeq r_0$, where r_0 is the initial orbital separation. Note that most of the bending occurs for r not much larger than r_0. For $r = r_0$ equation (12) reads then

$$\frac{du_p}{dz} = A \left[\frac{r_0}{(r_0^2 + z^2)^{1/2}} - u_p \right]^2 \frac{z}{r_0^2 + z^2}, \tag{14}$$

The solution near the origin, when $u_p \ll 1$ is

$$u_{p0}(r \sim r_0) \simeq \frac{A}{2} \frac{z^2}{r_0^2 + z^2}. \tag{15}$$

The asymptotic velocity is reached when the numerical value inside the square brackets in equation (14) is very small, or

$$u_{pac}(r \sim r_0) \simeq \frac{r_0}{(r_0^2 + z^2)^{1/2}}. \tag{16}$$

The change of behavior between the solution near the jets' origin and the asymptotic solution takes place when $u_{p0} \sim u_{pa}$, which by equations (15) and (16) is

$$u_{pac} \sim \left(1 + \frac{1}{A^2} \right)^{1/2} - \frac{1}{A}. \tag{17}$$

This very crude expression for the asymptotic transverse velocity is drawn by a thin line on Figure 3.

As the jet leaves the launching accretion disk, it is very dense and no bending occurs, namely, du_p/dz is very small. At large distances from the jet's origin, the angle δ is small and bending is no longer efficient. The bending is most efficient at some intermediate value of z, after the density of the jets decreases as they expand, but before the angle δ decreases much. Practically, this intermediate value of z is quite close to the jet's origin, $z \lesssim r_0$, as is seen in the lower panel of Figure 2.

If the jet pair in a binary system is known to be blown in a time period much shorter than the orbital period (an impulsive jet pair), and a bending is observed, the bending angle can be used with the thick line in Figure 3 to find the constant A given in equation (9). Thus the relation between the three quantities: the primary stellar mass loss rate $\dot{M}_s$, the secondary stellar mass loss rate to the two jet $\dot{M}_j$, and the half opening angle of the jets α, can be found.
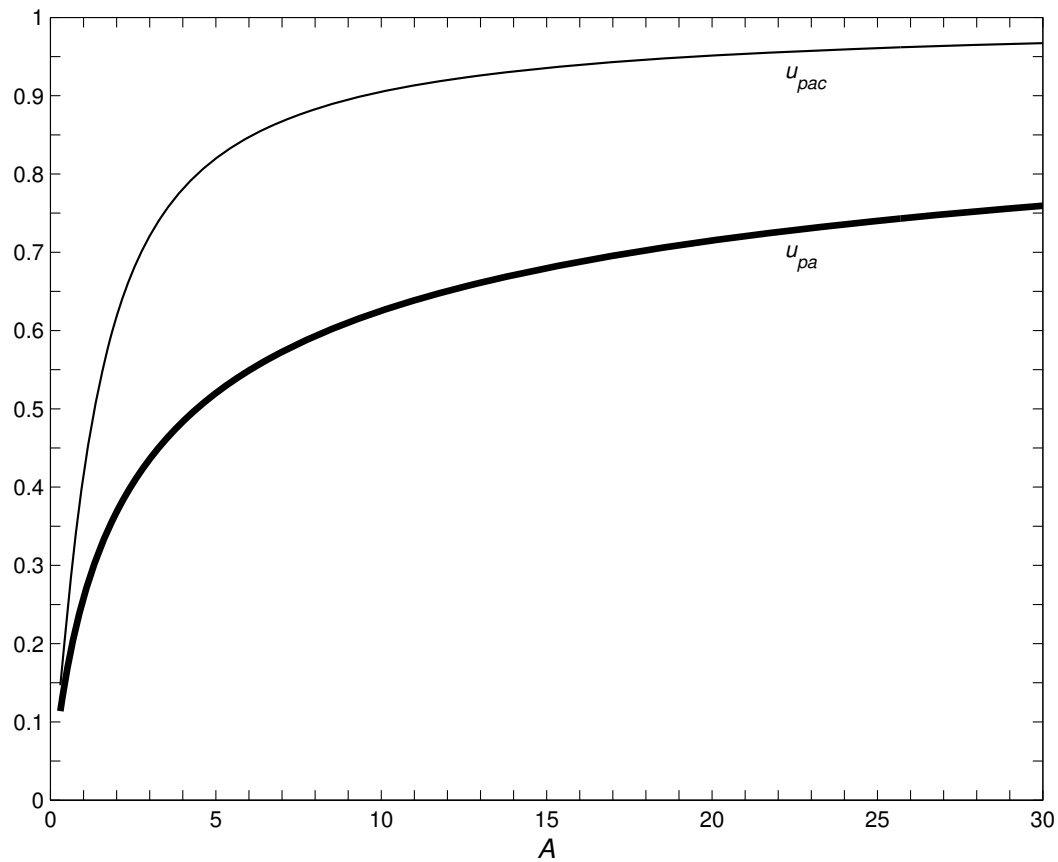
Fig. 3.— The asymptotic transverse velocity of u_p, u_{pa}, as function of the factor A (eq. 9) is depicted by the thick line. The thin line is the crude approximate equation for the asymptotic transverse velocity as given by equation (17).

3.   BENDING IN CLUSTERS

Many jet pairs blown by radio galaxies are observed to be bent as a result of the relative motion of the galaxy and the ICM (e.g., Bliton et al. 1998). Radio jets which are strongly bent are called narrow-angle tailed (NAT) radio galaxies, while those with slightly bent jets are called wide-angle tailed (WAT) radio galaxies. Many of the WAT radio galaxies are dominant galaxies in clusters, like cD galaxies (Owen & Rudnick 1976; Burns et al. 1979). A bulk motion of the IC, e.g., as a result of cluster merger, can efficiently bend radio jets (Bliton et al. 1998). A bulk ICM motion relative to the central cD galaxy can exist as a result of merging with a sub-cluster (group of galaxies), as found in several cases (Dupke & Bregman 2005, 2006; Fujita et al. 2006).

The bending process of jets by the ICM was extensively studied (e.g. Balsara & Norman 1992); the calculations are not repeated here. Basically, the bending of jets in clusters is characterized by the curvature radius R_c of the bent jet. Because the ambient density changes slowly with distance from the cluster center, unlike the case in PNs, a constant ambient density is assumed in the region where most of the jet's bending occurs. An approximate expression for the radius of curvature is (Sarazin et al. 1995)

$$R_{\mathrm{curv}} \sim 2 \left(\frac{L_{2j}}{3 \times 10^{43} \text{ erg s}^{-1}} \right) \left(\frac{R_j}{1 \text{ kpc}} \right)^{-1} \left(\frac{v_j}{0.1c} \right)^{-1} \left(\frac{v_a}{300 \text{ km s}^{-1}} \right)^{-2} \left(\frac{n_e}{0.1 \text{ cm}^{-3}} \right)^{-1} \text{ kpc} \tag{18}$$

where n_e is the ambient electron density, R_j is the jet's radius where most bending takes place, the total mechanical (kinetic) power of the two jets, L_{2j}, was scaled according to Birzan et al. (2004), and the relative ambient to jet speed v_a according to Malumuth (1992), with a 90° angle between the initial jet velocity and the ambient flow. To achieve a noticeable bending in cD clusters we require $R_{\mathrm{curv}} \lesssim 10$ kpc. This implies that even if the relative velocity of the cD galaxy to the ambient medium component perpendicular to the jet axis is ~ 100 km s^{-1} we get the required bending, as observed in some jets, or bubbles, blown by cD galaxies. This required bending will occur also for a narrower jet or a faster jet with v_j close to the speed of light c,

Our primary interest is to compare the bending process in binary stars to that of jets blown by the dominant cD galaxies at the centers of cooling flow clusters (or galaxies). Common to bending of jets in binary progenitors of PNs (referred to as bending in PNs) and bending of jets at the centers of clusters of galaxies is that the jets are bent by the ram pressure due to the relative motion of the medium the jets expand to and interact with, both in PNs and clusters. This is unlike point-symmetric structures which result from precession; in both PNs and clusters precession is due to the accretion disk that launches the jets and not due to the ambient medium. There are some differences between bending in clusters and

bending in binary systems, such as PNs' progenitors.

1. *Relative velocity.* The bending considered in PNs is due to the outflow velocity of the slow wind blown by the primary star. This implies that the angle between the jets velocity and the ambient medium velocity, δ in Figure 1, decreases very fast. It decreases even if bending does not occur. In clusters the velocity is due to the motion of the cD galaxy relative to the ICM. The angle decreases only because of the bending, and it decreases slowly.

2. *Densities.* The jet's density decreases as the jet moves outward, both in clusters and in stellar binary systems. However, in PNs the density of the bending slow wind (see Fig. 1) decreases as well, $\rho_s \propto (r^2 + z^2)$ (denominator of last term in eq. 8), while near the center of clusters the ICM density profile is much shallower and decreases slowly with increasing distance.

3. *Asymmetry in clusters.* The bending process in PNs is the same for the two opposite jets, but this is not necessarily the case in clusters of galaxies. If the jets are not blown perpendicular to the relative velocity between the ICM and the galaxy, then the jet expanding to the same direction the galaxy moves to will feel a larger ram pressure opposing its expansion velocity, and it will be slowed down more efficiently. More important, as this jet is bent, the angle of the relative velocity between the ICM and the galaxy to the jet's axis will increase to 90° before decreasing. In the opposite jet this angle decreases continuously. Therefore, the jet expanding against the ICM motion will be bent more than the other jet. Asymmetry between the two jets in clusters can be also caused by the presence of asymmetric strong magnetic fields in the ICM (Soker 1997), and/or density inhomogeneities such as clouds (Sarazin et al. 1995).

4. *Late stages of the bending process.* After reaching their asymptotic bending angle ϕ, jets in binary stellar systems will not bend any more. If a jet inflates a bubble, it will move outward radially along the streaming slow wind material. In clusters the situation is different because of the flow structure mentioned in points (1) and (2) above and because the low density bubbles buoyant outward. The result is that although the radio jets of cD galaxies are not bent much, after they become subsonic the bending is very efficient (Eilek et al. 1984; Odea & Owen 1986), and the asymmetry between the two sides can substantially increase (Burns et al. 1986).

5. *The effective bending location.* From the differences in points 1,2, and 4 it turns out that in stellar binary systems most of the bending occurs close to the jets' origin (lower panel of fig. 2). In clusters the bending becomes more efficient as the jet expands and slows down. In particular, if the jet inflate bubbles, they move slowly, have very low

density, and large cross section. Thus, in clusters the departure from axisymmetry will be most noticeable in bubbles.

Despite the differences listed above, there are some striking morphological similarities of bubbles displaced from the symmetry axis in PNs and clusters; two cases are mentioned in §1 (see appendix of the astro-ph version of the paper).

4. SUMMARY

In recent years the jet shaping model for many PNs and similar objects, like the massive binary star η Carinae, acquired considerable acceptance. It should be stressed that not all PNs were shaped by jets, and not all morphological structure in PNs were formed by jets. Bubble pairs, though, are most likely inflated by double jets, and the jets are probably blown by a stellar secondary star. The secondary star accretes mass from the primary's slow wind, forms an accretion disk and blow two jets, either continuously or impulsively, that is, during a time shorter than the orbital period. In some PNs, the line joining the centers of the two bubbles in a pair does not pass through the center of the nebula, meaning that the bubbles are displaced such that the nebular structure departs from axisymmetry. The explanation is that the two jets that inflate the bubbles were bent to the same side by the ram pressure of the slow wind (Fig. 1).

We therefore set the goal of deriving a simple and approximate relation between the bending angle of the jets and the properties of secondary stellar jets and the primary slow wind. For fast jets, $v_j \gg v_s$, the important factor is the quantity A defined in equation (9). The relation between the jet's asymptotic transverse speed v_{pa} (see fig. 1) and A is presented by the thick line in Figure 3, and a very crude approximation is given in equation (17) (v_{pa} is in units of the slow wind speed v_s). If the jets are impulsive, then the bending will be easier to observe; otherwise it is averaged over different directions as the binary system rotate. If A is not too small, and the orientation of the nebula is such that the bending is not along the line of sight, then observations may reveal the two jets or the bubbles (lobes) inflated by the jets to be displaced to the same side of the symmetry axis. Examples of such PNs are listed and classified by Soker & Hadar (2002).

In some clusters, X-ray-deficient bubble (cavity) pairs that were inflated by jets blown by the central cD galaxy, show displacement from axisymmetry similar to visible-deficient bubble (lobe) pairs observed in PNs (see appendix of the astro-ph version of this paper). We therefore set a second goal of comparing the bending process of jets in these two groups of objects. Two factors of the bending process are common to these two classes of objects:

1) the bending results from the ram pressure perpendicular to the jet axis, and 2) the ram pressure is exerted by the same external medium the jets expand to and interact with.

However, there are some significant differences listed in §3. (1) Because the bending in binary systems results from the slow wind blown by the primary star, the ambient density decreases faster with distance than the ambient density of the ICM in the centers of clusters. (2) Also, the angle δ (see Fig. 1) between the jet velocity and ambient slow wind velocity in binary systems decreases with distance along the jet axis, even when bending does not occur. In clusters the relative velocity is due to the bulk ICM motion and changes only because of bending. (3) In binary systems the two opposite jets are likely to be blown perpendicular to the orbital plane, thus they will be bent in the same way. In clusters, the jets' axis need not be perpendicular relative to the bulk motion of the ICM relative to the central black hole that blows the jets, so the jet facing the ICM flow will be bent more efficiently. In binary systems such an asymmetry between the two jets can occur if the jets (more specifically the accretion disk that launches the jets) precess. (4) In clusters, after the bubbles (cavities; lobes) are inflated, they buoy outward. They are more susceptible than the jets to the ram pressure, and departure from axisymmetry may substantially increase. This process does not exist in binary systems because the circumbinary ambient matter is not in hydrostatic equilibrium, but rather the ambient matter expands at a high Mach number. (5) In binary stars most of the bending occurs when the jets are at a distance $z \lesssim r_0$, where r_0 is the orbital separation. In clusters the bending becomes more efficient at larger and larger distances.

We hope that the study presented in this paper will motivate researchers to pay more attention to the departure from axisymmetry of bubble (cavity; lobe) pairs in both clusters of galaxies and PNs.

REFERENCES

Arrieta, A., Torres-Peimbert, S., & Georgiev, L. 2005, ApJ, 623, 252

Balick, B., & Frank, A. 2002, ARA&A, 40, 439

Balick, B., & Hajian, A. R. 2004, AJ, 127, 2269

Balsara, D., & Norman, M. L. 1992, ApJ, 393, 631

Birzan, L., Rafferty, D. A., McNamara, B. R., Wise, M. W., & Nulsen, P. E. J. 2004, ApJ, 607, 800

Bliton, M.; Rizza, E.; Burns, J. O.; Owen, F. N.; Ledlow, M. J. 1998, MNRAS, 301, 609B

Burns, J. O., Gregory, S. A., Odea, C. P., & Balonek, T. J. 1986, ApJ, 307, 73

Burns, J. O., Owen, F. N., & Rudnick, L. 1979, AJ, 84, 1683

Corradi, R. L. M., Livio, M., Balick, B., Munari, U., & Schwarz, H. E. 2001, ApJ, 553, 211

Corradi, R. L. M., & Schwarz, H. E. 1995, A&A, 293, 871

Doyle, S., Balick, B., Corradi, R. L. M., & Schwarz, H. E. 2000, AJ, 119, 1339

Dunn, R. J. H., Fabian, A. C., & Sanders, J. S. 2006, MNRAS, in press astro-ph/0512022)

Dupke, R. A., & Bregman, J. N. 2005, ApJS, 161, 224

Dupke, R. A., & Bregman, J. N. 2006, ApJ, in press (astro-ph/0512045)

Eilek, J. A., Burns, J. O., Odea, C. P., Owen, F. N. 1984, ApJ, 278, 37

Fabian, A. C., et al. 2000, MNRAS, 318, L65

Feibelman, W. A., 1985, AJ, 90, 2550

Fujita, Y., Sarazin., C. L., & Sivakoff, G. R. 2006, PASJ, in press (astro-ph/0512308)

Galloway, D. K., & Sokoloski, J. L. 2004, ApJ, 613, L61

Garcia-Arredondo, F., & Frank, A. 2004, ApJ, 600, 992

Gieseking, F., Becker, I., & Solf, J. 1985, ApJ, 295, L17

Guerrero, M. A., Chu, Y.-H., Manchado, A., Kwitter, K. B. 2003, AJ, 125, 3213

Guerrero, M. A., Miranda, L. F., Chu, Y.-H., Rodriguez, M., & Williams, R. M. 2001, ApJ, 563, 883

Huggins, P. J., Muthu, C., Bachiller, R., Forveille, T., & Cox, P. 2004, A&A, 414, 581

Kastner, J. H., Balick, B., Blackman, E. G., Frank, A., Soker, N., Vrtilek, S. D., & Li, J. 2003, ApJ, 591, L37

Kellogg, E., Pedelty, J. A., & Lyon, R. G. 2001, ApJ, 563, L151

Lee, C.-F., & Sahai, R. 2003, ApJ, 586, 319

Lee, C.-F., & Sahai, R. 2004 ,ApJ, 606, 483

Livio, M., & Soker, N. 2001, ApJ, 552, 685

Malumuth, E. M. 1992, ApJ, 386, 420

McNamara, B. R., Nulsen, P. E. J., Wise, M. W., Rafferty, D. A., Carilli, C., Sarazin, C. L. & Blanton, E. L. 2005, Nature, 433 ,45

Meaburn, J. 2006, in 'Diffuse Matter from Star Forming Regions to Active Galaxies', Eds. T. W. Harquist, J. M. Pittard and S. A. E. G. Falle (astro-ph/0512099)

Miranda, L. F., Guerrero, M. A., & Torrelles, J. M. 2001a, MNRAS, 322, 195

Miranda, L. F., Torrelles, J. M., Guerrero, M. A., Vazquez, R., & Gomez, Y. 2001b, MNRAS, 321, 487

Morris, M. 1987, PASP, 99, 1115

Odea, C. P., & Owen, F. N. 1986, ApJ, 301, 841

Oppenheimer, B. D., Bieging, J. H., Schmidt, G. D., Gordon, K. D., Misselt, K. A., & Smith, P. S. 2005, ApJ, 624, 957

Owen, F. N., & Rudnick, L. 1976, ApJ, 205, L1

Parthasarathy, M., Garcia-Lario, P., Pottasch, S. R., de Martino, D., Surendiranath, R. 2000, A&A, 355, 720

Pena, M., Hamann, W.-R., Ruiz, M. T., Peimbert, A., & Peimbert, M. 2004, A&A, 419, 583

Pizzolato, F. & Soker, N. 2005, AdSpR, 36, 762 (astro-ph/0501658) (Paper-4)

Riera, A., Raga, A. C., & Alcolea, J. 2005, RMxAA, 41, 147

Sahai, R., Le Mignant, D., Sanchez Contreras, C., Campbell, R. D., & Chaffee, F. H. 2005, ApJ, 622, L53

Sahai, R., & Nyman, L.-A. 2000, ApJ, 538, L145

Sahai, R., & Trauger, J. T. 1998, AJ, 116, 1357

Sarazin, C. L., Burns, J. O., Roettiger, K., & McNamara, B. R. 1995, ApJ, 447, 559

Schwarz, H. E., Aspin, C., & Lutz, J. H. 1989, ApJ, 344, L29

Soker, N. 1990, AJ, 99, 1869

Soker, N. 1997, ApJ, 488, 572

Soker, N. 2002, ApJ, 568, 726

Soker, N. 2003a, Nature, 426, 236

Soker, N. 2003b, PASP, 115, 1296 (Paper-1)

Soker, N. 2004a, A&A, 414, 943 (Paper-2)

Soker, N. 2004b, NewA, 9, 285 (Paper-3)

Soker, N. 2004c, in Asymmetrical Planetary Nebulae III: Winds, Structure and the Thunderbird, eds. M. Meixner, J. H. Kastner, B. Balick, & N. Soker, ASP Conf. Series, 313, (ASP, San Francisco), p. 562 (see the extended version on astro-ph/0309228)

Soker, N. 2005, AJ, 129, 947

Soker, N., & Hadar, R. 2002, MNRAS, 331, 731

Soker, N., & Livio M. 1994, ApJ, 421, 219

Soker, N., & Rappaport, S. 2000, ApJ, 538, 241

Terzian, Y., & Hajian, A. R. 2000, "Asymmetrical Planetary Nebulae II: From Origins to Microstructures," eds. J.H. Kastner, N. Soker, & S. Rappaport, ASP Conf. Ser. Vol. 199, p. 33 (see PNs images at: http://ad.usno.navy.mil/pne/gallery.html)

Velazquez, P. F., Riera, A., & Raga, A. C. 2004, A&A, 419, 991

Vinkovic, D., Blöcker, T., Hofmann, K.-H., Elitzur, M., & Weigelt, G. 2004, MNRAS, 352, 852

Vrtilek, J. M., Grego, L., David, L. P., Ponman, T. J., Forman, W., Jones, C., & Harris, D. E. 2002, APS, APRB, 17107

APPENDIX

In this *appendix* we summarize the morphological similarities between X-ray deficient bubbles (cavities) in clusters or groups of galaxies and visible-light deficient bubbles (lobes) in PNs. The Table below is based on that given in Paper-1, with some additional comparisons. In Paper 1, Soker also pointed out similar values of some non-dimensional quantities between clusters and PNs. These similarities led Soker to postulate a similar formation mechanism, thereby strengthening models for PN shaping by jets, although not all PNs are shaped by jets; the jets in PN progenitors are likely blown by binary companions.

The images of the objects listed in Table 1 of Paper-1 are summarized in a *PowerPoint* file Soker presented at the Asymmetrical Planetary Nebulae III meeting (2003) at http://www.astro.washington.edu/balick/APN/APN_talks_posters.html go the 'ppt' file in the "Discussion" of Session 13. Other images were added here. All image sources are listed, and references not in the list of the paper are listed after the table.

Comments to the table in the *Appendix*:

(1) Similar images of bubbles in clusters of galaxies and planetary nebulae (PNs). In clusters these are X-ray images (e.g., with X-ray deficient bubbles), while in PNs they are visible-light images (e.g., with visible-light deficient bubbles). In the first eight pairs of images the similarity is of high degree. In the last two pairs of images the similarity between the cluster and the PN is of lesser degree.

(2) See Pizzolato & Soker (2005) for more detail.

(3) The low-resolution image of the same object is from the catalogue of Schwarz et al. (1992)

(4) Free access to images are at these sites:

[1] http://arxiv.org/PS_cache/astro-ph/pdf/0210/0210054.pdf

[2] http://ad.usno.navy.mil/pne/images/rob22.jpg

[3] http://arxiv.org/PS_cache/astro-ph/pdf/0007/0007456.pdf

[4] http://arxiv.org/PS_cache/astro-ph/pdf/0303/0303056.pdf

[5] http://arxiv.org/PS_cache/astro-ph/pdf/0107/0107221.pdf

[6] http://ad.usno.navy.mil/pne/images/vv171.jpg

[7] http://arxiv.org/PS_cache/astro-ph/pdf/0010/0010450.pdf

[8] http://ad.usno.navy.mil/pne/images/he2_104.jpg

[9] http://chandra.harvard.edu/photo/cycle1/hcg62/index.html

[10a] http://arxiv.org/PS_cache/astro-ph/pdf/0009/0009396.pdf
    see also: [10b] http://ad.usno.navy.mil/pne/images/hu21_ha.gif

[11] http://arxiv.org/PS_cache/astro-ph/pdf/0411/0411553.pdf

[12] http://ad.usno.navy.mil/pne/images/hb5.jpg

[13] http://ad.usno.navy.mil/pne/images/ngc6886.jpg

[14] http://arxiv.org/PS_cache/astro-ph/pdf/0001/0001402.pdf

[15] http://ad.usno.navy.mil/pne/images/ngc6537.jpg

[16] http://www.journals.uchicago.edu/ApJ/journal/issues/ApJ/
    v565n1/54312/54312.web.pdf

[17a] http://ad.usno.navy.mil/pne/images/ngc7009.jpg
    see also (Goncalves et al. 2004, fig. 1):

[17b] http://arxiv.org/PS_cache/astro-ph/pdf/0307/0307265.pdf

[18] http://chandra.harvard.edu/photo/2003/perseus/perseus_ripple_illustration_nolabel.jpg

[19] http://www.spitzer.caltech.edu/Media/releases/ssc2005-07/ssc2005-07a.shtml

Table 1.

Structure	Clusters	PNs
Butterfly shape; faint along symmetry axis[1]	Abell 478 [1][4] (Sun et al. 2003)	Roberts 22 [2] (Sahai et al. 1999)
Pairs of fat spherical bubbles near center	Perseus [3] (Fabian et al. 2000)	NGC 3587 [4] (Guerrero et al. 2003)
Closed bubbles connected at the equatorial plane	Abell 2052 [5] (Blanton et al. 2001)	VV 171 [6] (Sahai 2001)
Open bubbles connected at the equatorial plane	M 84 (Finoguenov & Jones 2001) [7]	He 2-104 (Sahai & Trauger, 1998) [8]
Pair of bubbles detached from a bright center	HCG 62 [9] (Vrtilek et al. 2002)	Hu 2-1 [10] (Miranda et al. 2001b)
Point symmetry; suggesting precession[2]	MS 0735.6+7421 [11] (McNamara et al. 2005)	Hb 5 [12][3] (Terzian & Hajian 2000)
Bending to one side	HCG 62 [9] (Vrtilek et al. 2002)	NGC 6886 [13] (Terzian & Hajian 2000)
point-symmetric elongated lobes	Hydra A [14] (McNamara et al. 2000)	NGC 6537 [15] (Balick 2000)
Pairs of bright bullets along the symmetry axis	Cygnus A [16] (Smith et al. 2002)	NGC 7009 [17] (Balick et al. 1998)
Ripples	Perseus [18] (Fabian et al. 2003;06)	M 57 (NGC 6720) [19] (Hora et al. 2005)

REFERENCES

Balick, B. 2000, "Asymmetrical Planetary Nebulae II: From Origins to Microstructures," eds. J.H. Kastner, N. Soker, & S. Rappaport, ASP Conf. Ser. Vol. 199, p. 41

Balick, B., Alexander, J., Hajian, A. R., Terzian, Y., Perinotto, M., & Patriarchi, P. 1998, AJ, 116, 360

Blanton, E. L., Sarazin, C. L., McNamara, B. R., & Wise, M. W. 2001, ApJ, 558, L15

Fabian, A. C., Sanders, J. S., Allen, S. W., Crawford, C. S., Iwasawa, K., Johnstone, R. M., Schmidt, R. W., & Taylor, G. B. 2003, MNRAS, 344, L43

Fabian, A. C., Sanders, J. S., Taylor, G. B., Allen, S. W., Crawford, C. S., Johnstone, R. M., & Iwasawa, K., 2006, MNRAS, in press (astro-ph/0510476)

Finoguenov, A., & Jones, C. 2001, ApJ, 547, L107

Goncalves, D. R., Mampaso, A., Corradi, R. L. M., Perinotto, M., Riera, A., & Lopez-Martin, L. 2004, MNRAS, 355, 37

Hora, J. L., Latter, W. B., Marengo, M., Fazio, G. G., Allen, L. E., & Pipher, J. L. 2005, AAS, 206, 3901

McNamara, B. R., et al. 2000, ApJ, 534, L135

Sahai, R. 2001, in Galactic Structure, Stars and the Interstellar Medium, Eds. Charles E. Woodward, Michael D. Bicay, and J. Michael Shull, ASP Conf. Ser. Vol. 231 (San Francisco: ASP), 528

Sahai, R., Zijlstra, A., Bujarrabal, V., Te Lintel Hekkert, P. 1999, AJ, 117, 1408

Schwarz, H. E., Corradi, R. L. M., & Melnick, J. 1992, A&A Suppl. Ser., 96, 23.

Smith, D. A.; Wilson, A. S., Arnaud, K. A., Terashima, Y., & Young, A. J. 2002, ApJ, 565 195

Sun, M., Jones, C., Murray, S. S., Allen, S. W., Fabian, A. C., & Edge, A. C. 2003, ApJ, 587, 619
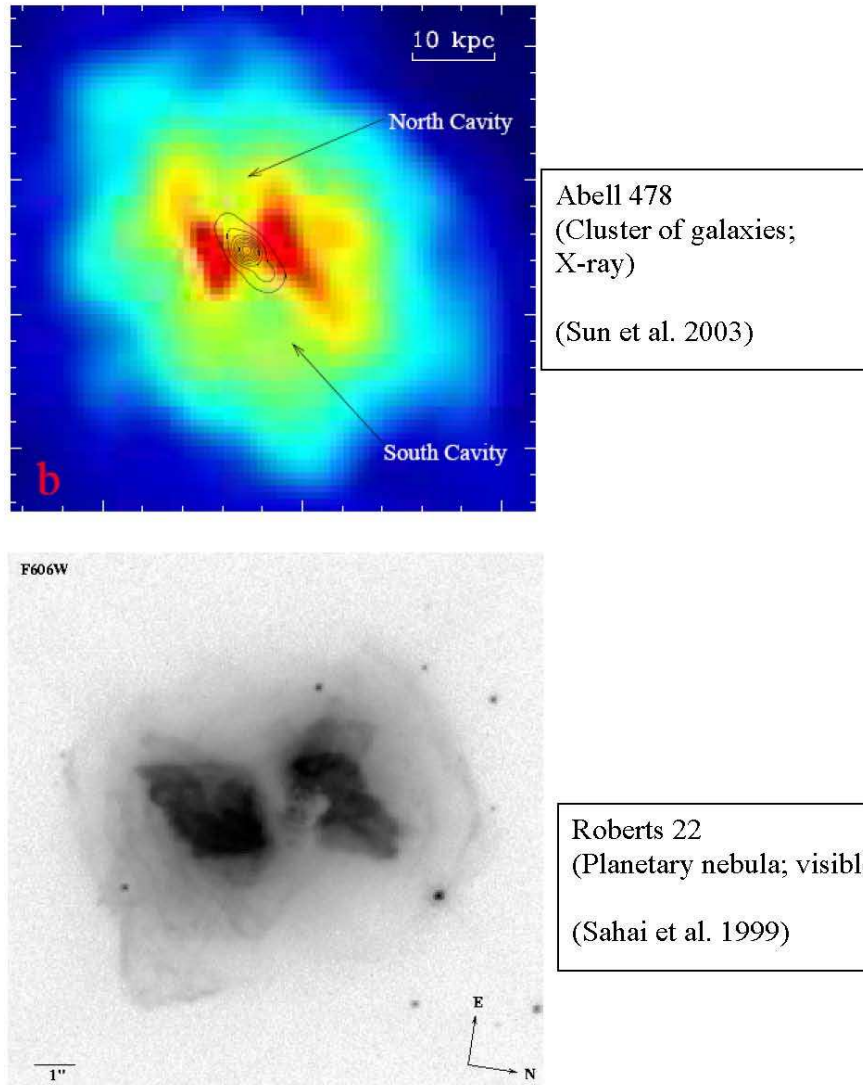
Fig. 4.— Comparing false color X-ray image of a galaxy cluster with a visible image of a planetary nebula, emphasizing the butterfly shape and a faint region along the symmetry axis.
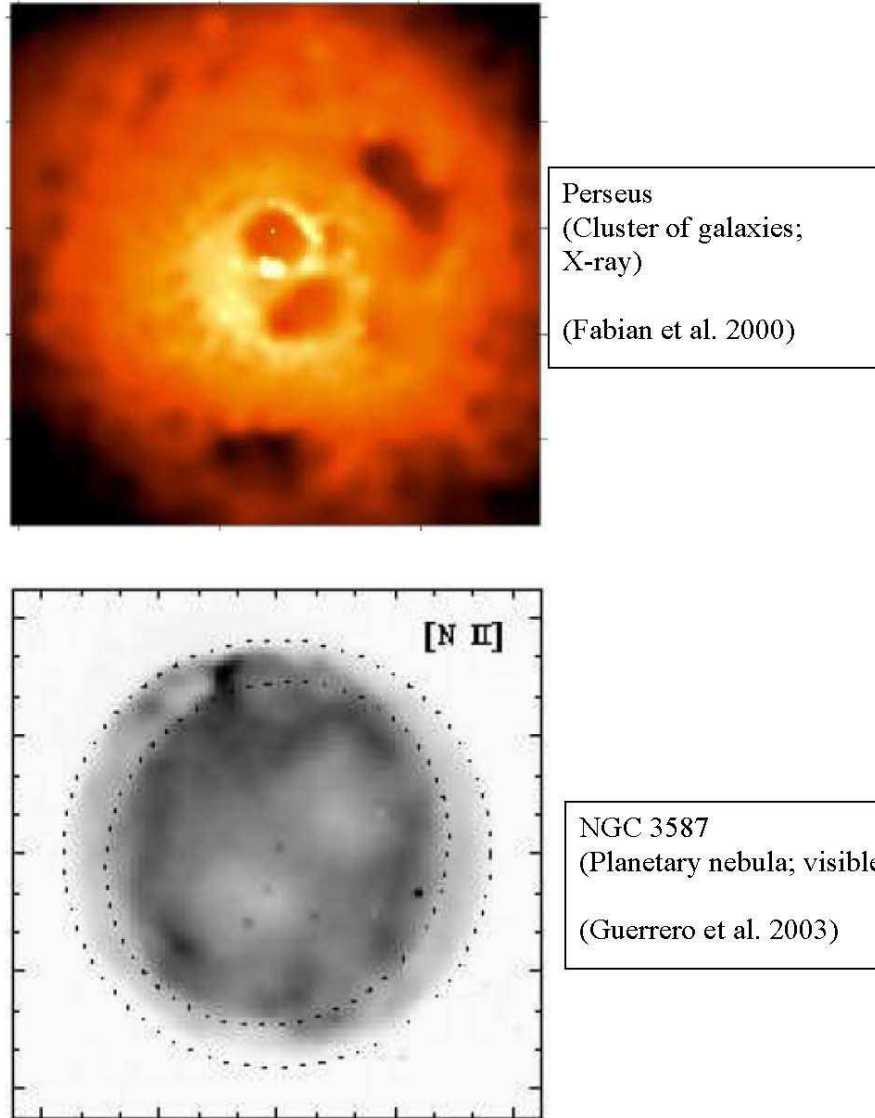
Perseus
(Cluster of galaxies;
X-ray)

(Fabian et al. 2000)

[N II]

NGC 3587
(Planetary nebula; visible)

(Guerrero et al. 2003)

Fig. 5.— Like Figure 4 but emphasizing pairs of fat spherical bubbles near the center.

Abell 2052
(Cluster of galaxies;
X-ray + visible contours)
(Blanton et al. 2001)

VV 171
(Planetary nebula; visible)

(Sahai 2001)
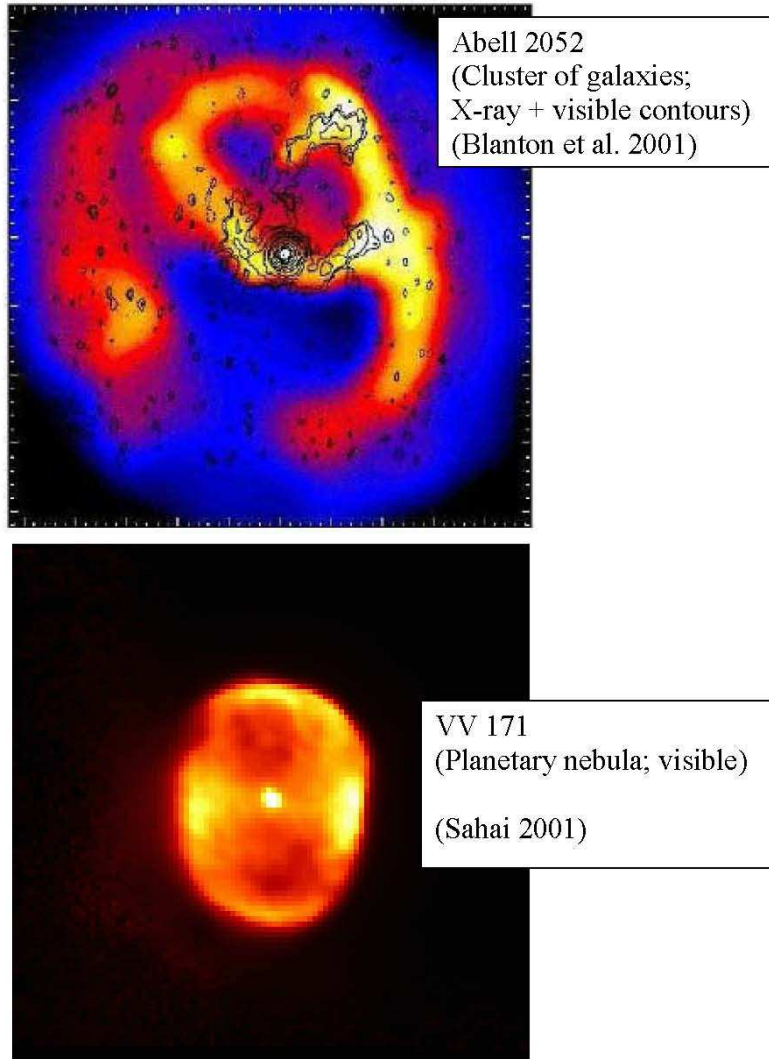
Fig. 6.— Like Figure 4 but emphasizing closed bubbles connected at the equatorial plane.

M 84   (Elliptical galaxy;
X-ray + radio contours)
(Finoguenov & Jones 2001)

He 2-104
(Planetary nebula;
visible)

(Sahai & Trauger
1998)
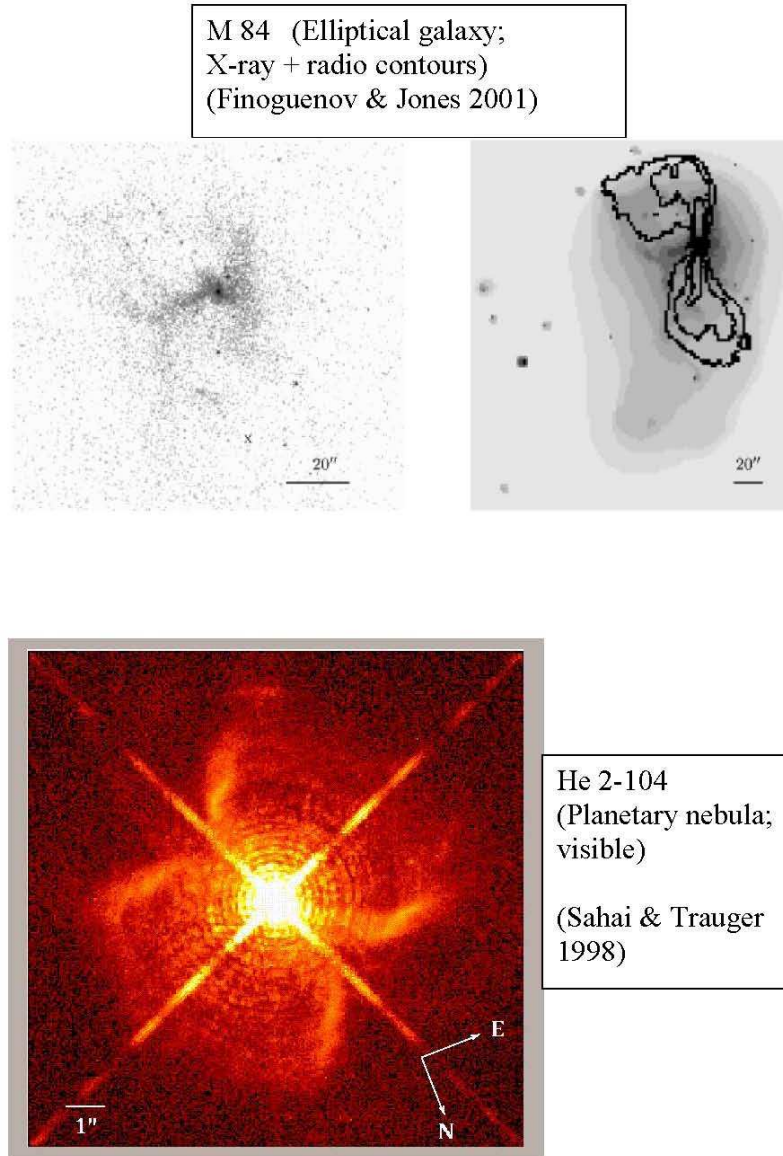
Fig. 7.— Like Figure 4 but emphasizing open bubbles connected at the equatorial plane.

HCG 62
(Galaxy group;   X-ray)

(Vrtilek et al. 2002)

Hu 2-1
(Planetary nebula;
visible)

(Miranda et al. 2001)
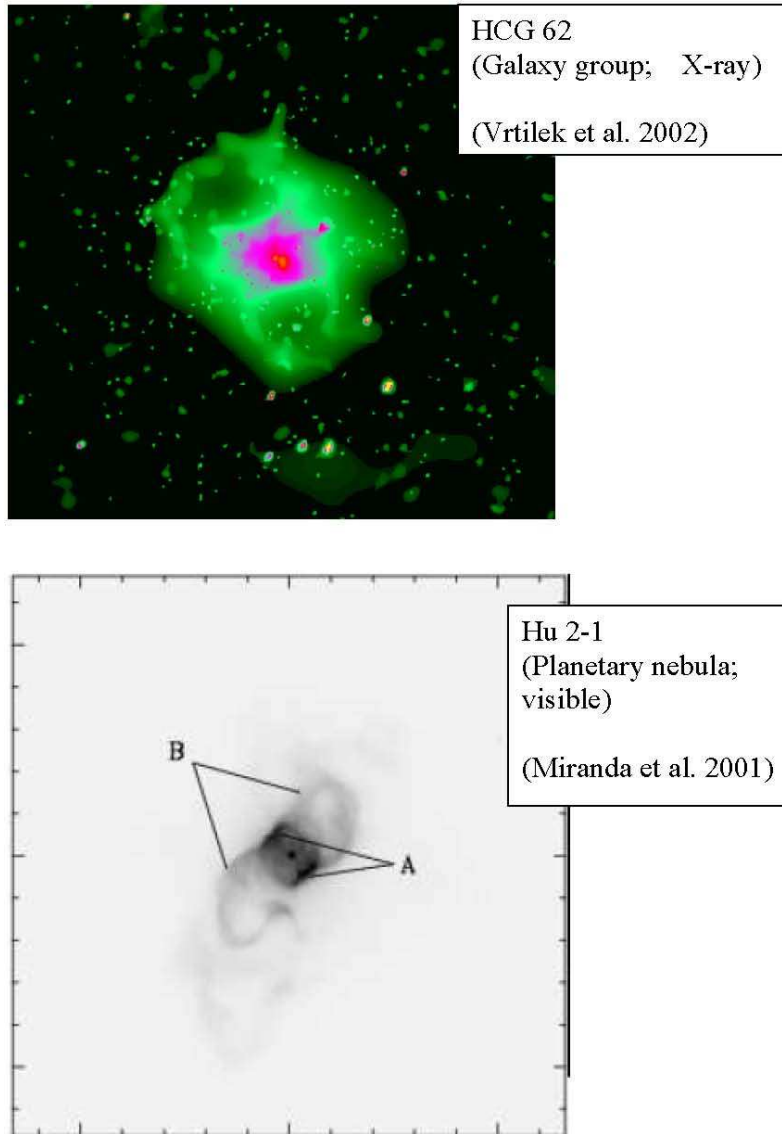
Fig. 8.— Like Figure 4 but emphasizing a bubble pair detached from a bright center .

MS0735.6+7421
(Galaxy cluster;
X-ray + radio contours)

(McNamara et al. 2005)

Hb 5
(Planetary nebula; visible)

(Terzian & Hajian 2000;   Schwarz et al. 1992)

Fig. 9.— Like Figure 4 but emphasizing point symmetry.

HCG 62
(Galaxy group;   X-ray)

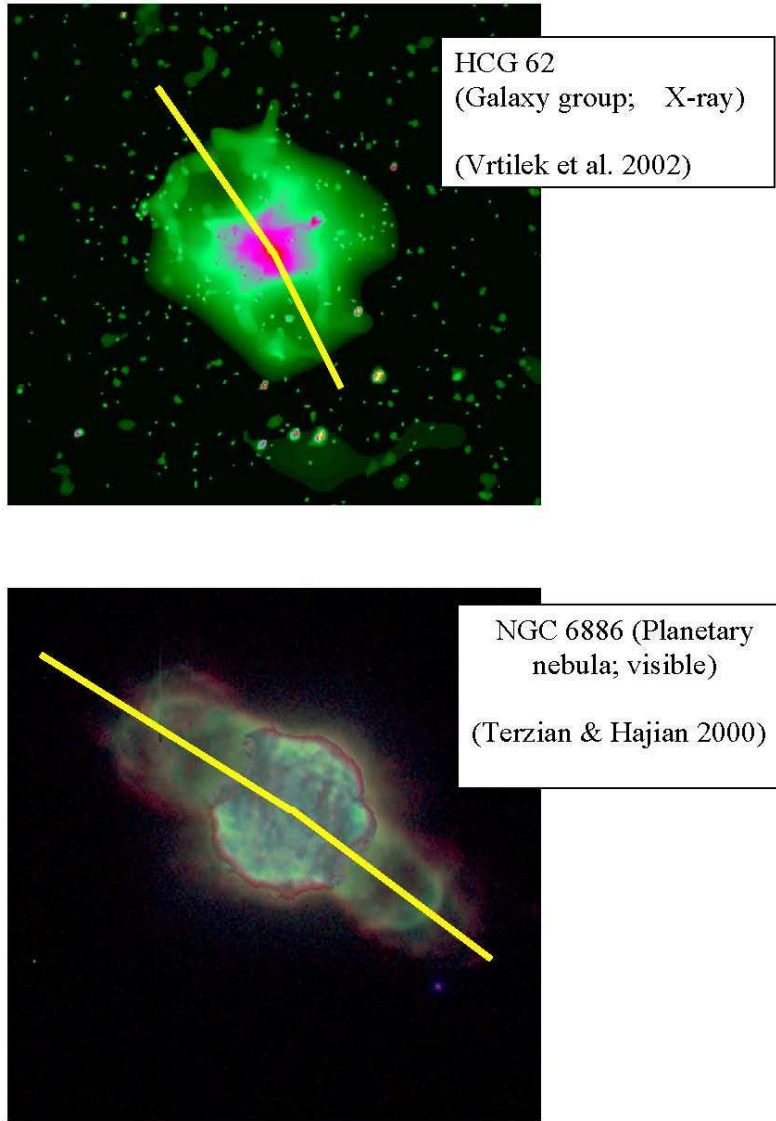(Vrtilek et al. 2002)

NGC 6886 (Planetary
nebula; visible)

(Terzian & Hajian 2000)
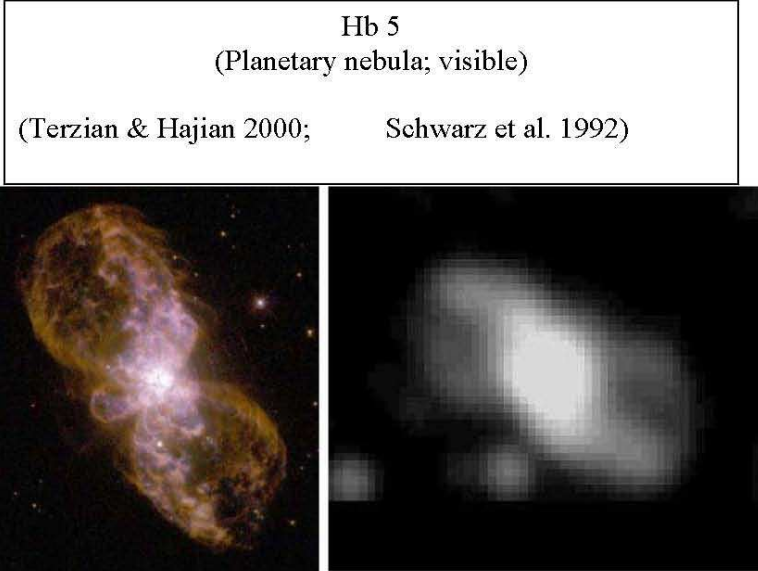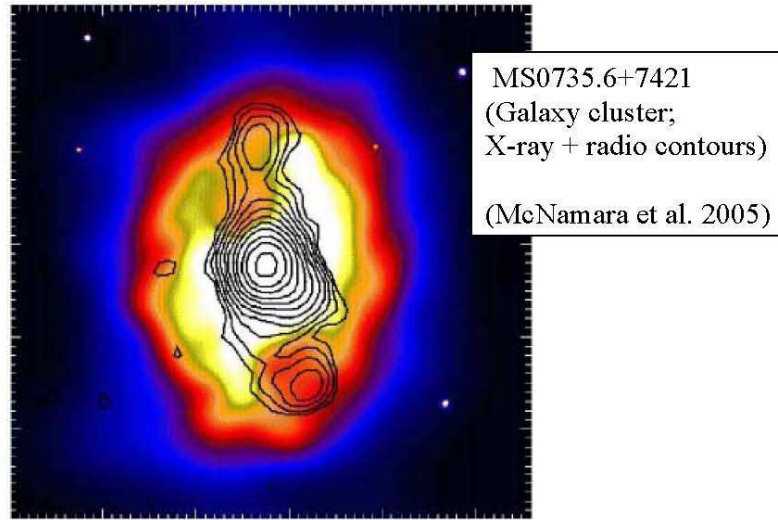
Fig. 10.— Like Figure 4 but emphasizing bending both bubbles (cavities; lobes) to one side (departure from axisymmetry).

Hydra A
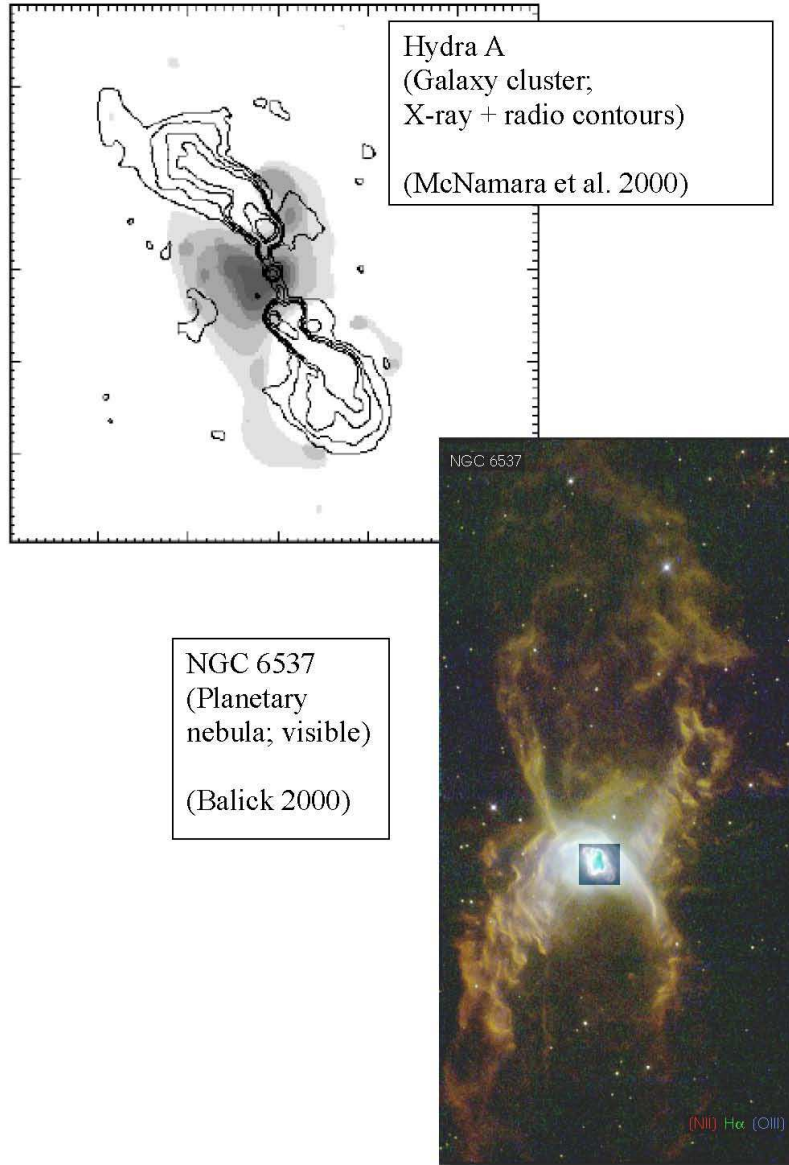(Galaxy cluster;
X-ray + radio contours)

(McNamara et al. 2000)

NGC 6537
(Planetary
nebula; visible)

(Balick 2000)

Fig. 11.— Like Figure 4 but emphasizing point-symmetric elongated lobes.

Cygnus A
(Galaxy cluster;   X-ray)

(Smith et al. 2002)

NGC 7009 (Planetary
nebula; visible)

(Balick et al. 1998)
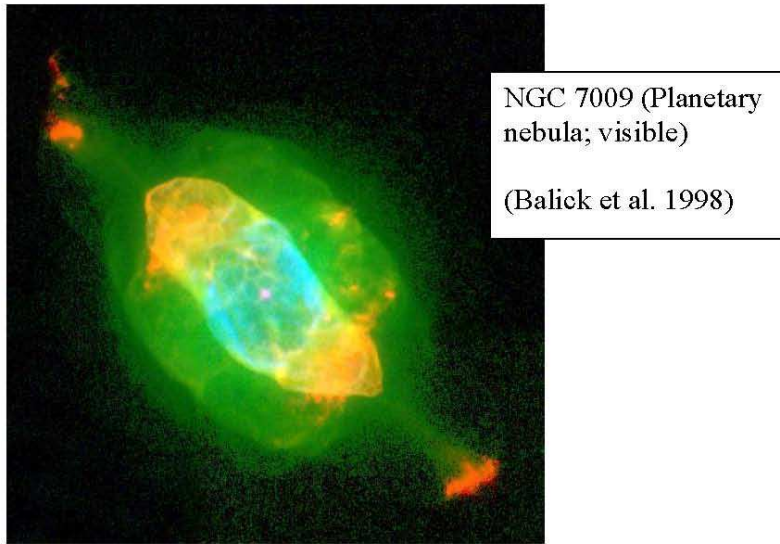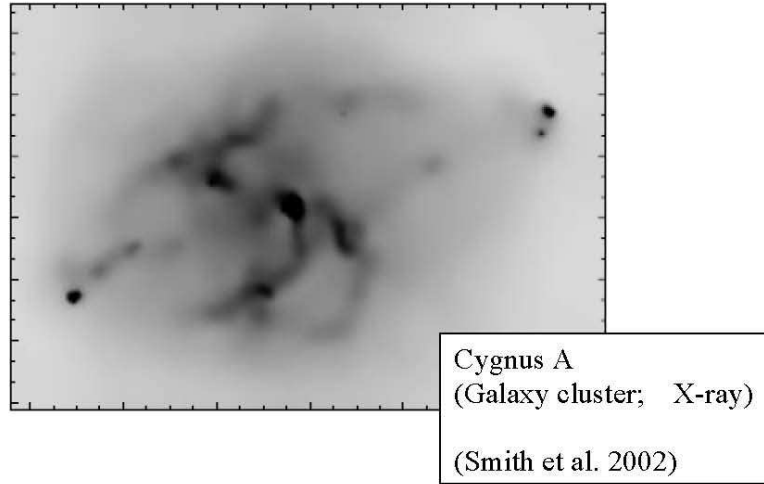
Fig. 12.— Like Figure 4 but emphasizing pairs of bright bullets along the symmetry axis.

Perseus
(Galaxy cluster;   X-ray)

(Fabian et al. 2003, 2006)

M 57 (NGC 6720) (Planetary nebula; visible + IR)
(Hora et al. 2005)

Ring Nebula/Messier 57   Spitzer Space Telescope • IRAC
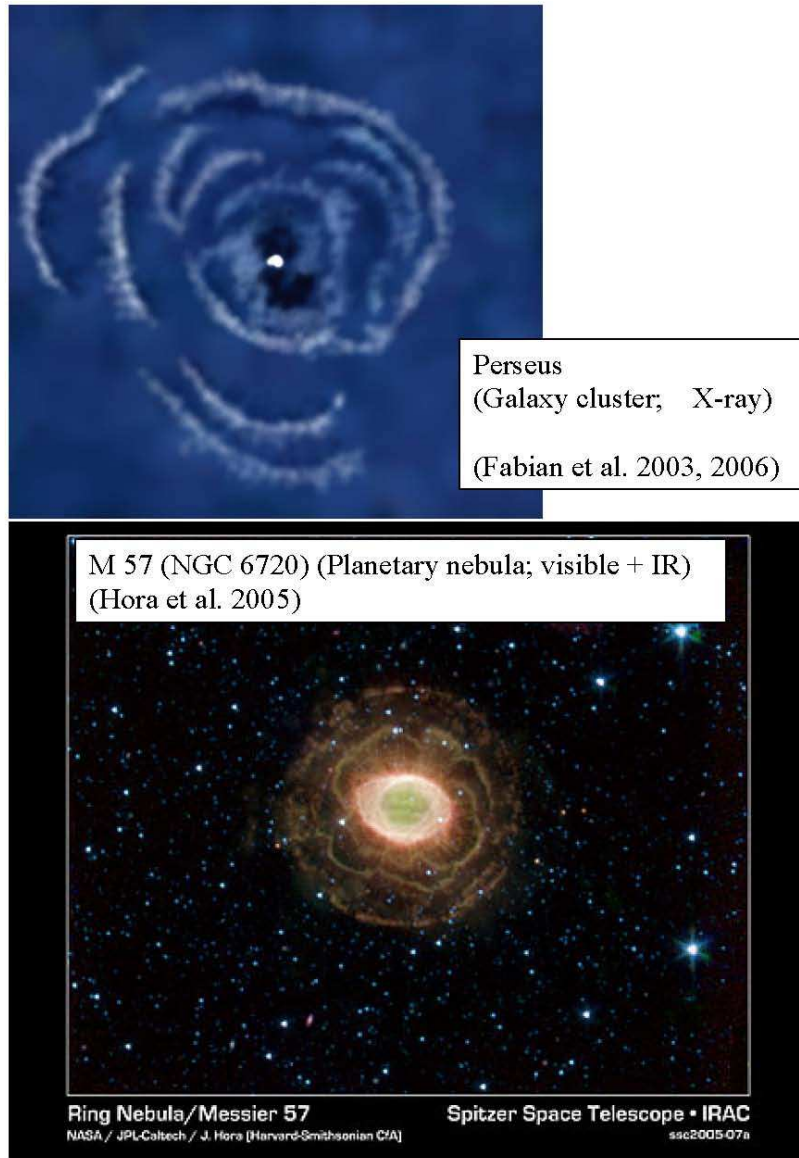NASA / JPL-Caltech / J. Hora [Harvard-Smithsonian CfA]   ssc2005-07a

Fig. 13.— Like Figure 4 but emphasizing ripples.